An ab Initio CFF93 All-Atom Force Field for Polycarbonates

Huai Sun, Stephen J. Mumby, Jon R. Maple, and Arnold T. Hagler*

Contribution from the Biosym Technologies, Inc., 9685 Scranton Road, San Diego, California 92121

*Received March 29, 1993. Revised Manuscript Received November 29, 1993**

Abstract: An all-atom CFF93 force field for polycarbonates based on *ab initio* calculations is reported. Force field parameters are derived by fitting to quantum mechanical total energies, first and second derivatives of total energies, and electrostatic potentials, all generated from *ab initio* quantum mechanical calculations on model compounds at HF/6-31G* level of theory. Valence parameters and *ab initio* charges are then scaled to correct for differences between experiment and the Hartree–Fock approximation. The van der Waals parameters and the scaling factors for atomic partial charges are determined from crystal structures. Based on the force field, molecular mechanics calculations are performed for several model compounds, and the results are compared with experimental values and with the results of the *ab initio* calculations.

1. Introduction

Although the quantum mechanical *ab initio* HF/6-31G* calculations[1] agree with most of the geometrical parameters measured experimentally, the conformational energies calculated suffer discrepancies in several places. A typical example is the barrier height for phenyl ring rotations. The *ab initio* calculations predict a barrier height of some 2 kcal/mol if the rings rotate synchronously, but dynamic ^{13}C NMR studies[2] reveal that the activation energy of this process is about 12 kcal/mol in glassy bisphenol a polycarbonate (BPAPC). Furthermore, this value of 12 kcal/mol agrees well with activation energies determined for the γ-relaxation of BPAPC by dynamic mechanical spectroscopy[3,4] and dielectric[5] studies. In order to redress the differences between the theoretical predictions and experimental observations, two points require attention: (1) the accuracy of the theoretical calculations and (2) the comparison of properties calculated for isolated molecules with those measured for molecules in a condensed phase. The accuracy of *ab initio* calculations has been extensively tested in terms of basis sets and electronic correlation for these molecules[1] and many others.[6] It is hard to relate such a large difference (more than 10 kcal/mol) to the approximations employed in the calculations (Hartree–Fock approximation and its correction based on the second-order Møller–Plesset perturbation theory and basis set dependence). Consequently, one might speculate that it is the problem of comparing calculations on isolated molecules with condensed phase measurements that is responsible in large part for the discrepancy.

In order to understand the differences between isolated molecules and molecules in a condensed phase, one needs an accurate force field, which includes both intra- and intermolecular interactions. In this sense, the force field plays the role of a bridge that connects theory to experiment, and the properties of isolated small molecules to those of structurally similar larger molecules in a condensed phase. Based on a realistic force field, one can conduct computer simulations such as molecular mechanics (MM), molecular dynamics (MD), or Monte Carlo (MC) studies to investigate the statistical behavior of a large number of molecules and relate the properties to those experimentally measured.

There is an increasing interest in force field development in recent years.[7-12] For polycarbonates in particular, several force fields have been developed. Early work[13] in this area was based on very limited experimental data. The rigid body assumption was used, and only nonbonded parameters were developed. Later, with additional crystal data for diphenyl carbonate, Tonelli,[14] Erman et al.,[15] and Sundararajan[16] developed several improved force fields by including some single bond rotations, but the carbonate group was still assumed to be all trans and no electrostatic interactions were considered. Very recently, Hutnik, Argon, and Suter[17] developed a classical force field based on the latest published experimental and theoretical results, which allows for rotations about all single bonds and includes both van der Waals nonbonded and electrostatic interactions, but the bond lengths and angles were still fixed.

In this paper, we report an all-atom force field, which is parameterized based on the *ab initio* HF/6-31G* calculations.[1] The method that we used to parameterize the force field differs from previous work[7-17] in that it first involves deriving a "quantum force field" obtained by fitting the quantum energy surfaces of a group of molecules containing the functional group of interest, described by the *ab initio* energies, first and second derivatives of the energies and electrostatic properties. In the second step, the quantum mechanical force field is scaled by parameters derived by fitting experimental data for a large number of organic compounds.[18]

* Abstract published in *Advance ACS Abstracts*, January 15, 1994.

(1) Sun, H.; Mumby, S. J.; Maple, J. R.; Hagler, A. T. Submitted to *J. Phys. Chem.*

(2) Roy, A. K.; Jones, A. A.; Inglefield, P. T. *Macromolecules* **1986**, *19*, 1356.

(3) Yee, A. F.; Smith, S. A. *Macromolecules* **1981**, *14*, 54.

(4) Khanna, Y. P. J. *Thermal Anal.* **1985**, *30*, 153.

(5) Shih, K. S.; Beatty, C. L. *Polym. Eng. Sci.* **1987**, *27*, 440.

(6) Hehre, W. J.; Radom, L.; Schleyer, P. v. R.; Pople, J. A. *Ab initio Molecular Orbital Theory*, John Wiley & Sons: New York, 1986; and references therein.

(7) Weiner, S. J.; Kollman, P. A.; Ngnyen, D. T.; Case, D. A. *J. Comput. Chem.* **1986**, *7*, 230.

(8) Dauber-Osguthorpe, P.; Roberts, V. A.; Osguthorpe, D. J.; Wolff, J.; Genest, M.; Hagler, A. T. *Proteins: Structure, Function and Genetics* **1988**, *4*, 31.

(9) Nilsson, L.; Karplus, M. *J. Comput. Chem.* **1990**, *7*, 591.

(10) Allinger, N. L.; Rahman, M.; Lii, J. *J. Am. Chem. Soc.* **1990**, *112*, 8293.

(11) Rappé, A. K.; Casewit, C. J.; Colwell, K. S.; Goddard, W. A.; Skiff, W. M. *J. Am. Chem. Soc.* **1992**, *114*, 10024.

(12) Amodeo, P.; Barone, V. *J. Am. Chem. Soc.* **1992**, *114*, 9085.

(13) Williams, A. D.; Flory, P. J. *J. Polym. Sci., Polym. Phys. Ed.* **1968**, *6*, 1945.

(14) Tonelli, A. E. *Macromolecules* **1972**, *5*, 558.

(15) Erman, B.; Marvin, D. C.; Irvine, P. A.; Flory, P. J. *Macromolecules* **1982**, *15*, 664.

(16) Sundararajan, P. R. *Can. J. Chem.* **1985**, *63*, 103.

(17) Hutnik, M.; Argon, A. S.; Suter, U. W. *Macromolecules* **1991**, *24*, 5956; 5970.

(18) Maple, J. R.; Dinur, U.; Hagler, A. T. *Proc. Natl. Acad. Sci. U.S.A.* **1988**, *85*, 5350. Maple, J. R.; Hwang, M.-J.; Stockfisch, T. P.; Dinur, U.; Waldman, M.; Ewig, C. S.; Hagler, A. T. *J. Comput. Chem.*, in press.

0002-7863/94/1516-2978$04.50/0

Because *ab initio* calculations can provide much more and detailed information for the molecular interactions, the resulting force field from this approach is more general than those developed for these functional groups previously.[13-17] Since all degrees of freedom are considered, the resulting force field may be used to derive not only structural and energetic properties but also detailed information regarding inter- and intramolecular motions such as molecular vibrations. The importance of allowing molecular flexibility is suggested by the large variation in bond lengths and especially valence angles in the different conformations seen in the quantum mechanical analysis.[1] These coordinates thus seem to be coupled with the structural and energetic properties we seek. Because the nonbonded parameters were determined from both isolated molecule and solid-state calculations, the force field is useful for modeling molecules in both gas and condensed phases.

In the following sections, the procedure for developing such a force field is first briefly presented, the details of the calculation are given, and finally the validation of the force field against *ab initio* results and experimental data is described.

2. Method

The procedure used to develop the force field, which is described in detail elsewhere,[18] can be summarized briefly as follows. First, a number of model compounds are selected such that all possible intramolecular interactions are represented. Then the geometries of these model compounds are optimized by using *ab initio* molecular orbital methods with a selected basis set (6-31G* in this work[19]). The optimized geometries include not only global minima but also those local minima and transition states that are crucial to produce an accurate representation of the conformational energy surfaces. From those optimized structures, a complete sampling is obtained by randomly distorting each of the optimized structures along the normal mode coordinates. The extent of sampling is controlled by setting a cut-off energy to avoid very high-energy structures and by varying the number of distorted structures to ensure that a good representation of each internal degree of freedom has been obtained. Next, *ab initio* calculations are performed on each of these distorted structures. The total energies and their first and second derivatives (gradients and Hessians), dipole moments, and derivatives of dipole moments are obtained for each structure. All of these quantities are collected and used to fit the potential function, which is given as[18]

$$E = \sum E^{b} + \sum E^{a} + \sum E^{o} + \sum E^{t} + \sum E^{bb} + \sum E^{ab} + \sum E^{aa} + \sum E^{at} + \sum E^{bt} + \sum E^{elec} + \sum E^{VDW} \quad (1)$$

where

$$E^{b} = \sum_{i=2}^{4} k_i^{b}(b - b_o)^i$$

$$E^{a} = \sum_{i=2}^{4} k_i^{a}(\theta - \theta_o)^i$$

$$E^{t} = \sum_{i=1}^{4} k_i^{t}(1 - \cos i\,\phi)$$

$$E^{o} = k^{o}(\chi - \chi_o)^2$$

$$\{E^{bb}, E^{aa}, E^{ab}\} = k^{c}(s - s_o)(s' - s'_o) \quad (2)$$

$$\{E_{bt}\} = (b - b_o)\sum_{i=1}^{3} k_i^{c}(1 - \cos i\,\phi)$$

$$\{E_{at}\} = (\theta - \theta_o)\sum_{i=1}^{3} k_i^{c}(1 - \cos i\,\phi)$$

$$E^{el}{}_{cc} = \sum_{i,j} \frac{q_i q_j}{r_{ij}}$$

$$E^{VDW} = \sum_{i,j} \epsilon_{i,j}\left[2\left(\frac{r^{o}_{i,j}}{r_{ij}}\right)^{9} - 3\left(\frac{r^{o}_{i,j}}{r_{ij}}\right)^{6}\right]$$

The total energy is divided into three major categories: (a) contributions from each of the internal valence coordinates, (b) coupling or cross terms between two internal coordinates, and (c) nonbonded interactions. The valence energies consist of terms from distortions of bond lengths E^{b}, bond angles E^{a}, out-of-plane bending angles E^{o}, and torsion angles E^{t}. Both bond and angle terms contain anharmonic constants to quartic terms to characterize anharmonic features. The torsion function is represented by a symmetric Fourier expansion. The out-of-plane function is considered to be a simple harmonic function due to the symmetry of this motion in polycarbonates. E^{bb} is the cross term between two bonds with one common atom, E^{aa} refers to two angles with a common bond, E^{ab} represents the coupling between a bond and an angle in which the bond is one of the edges, E^{bt} stands for interactions between a bond and a dihedral angle of rotation about the bond, and E^{at} is the cross term for an angle and a torsion, the torsion is defined as the rotation about the interior bond of the angle. The nonbonded energies are interactions between pairs of atoms that are separated by at least two intervening atoms or that belong to different molecules. The nonbonded energies are subsequently divided into van der Waals interactions E_{VDW} and electrostatic interactions E_{elec}. A 6–9 Lennard–Jones function is used to represent the van der Waals forces, while the electrostatic interaction is written in the form of a standard Coulombic interaction with partial atomic charges. The deficiencies of using atomic point charges have been well recognized and discussed.[1,20-24] As has been shown,[1] one can significantly improve the quality of representing electrostatic field by adding atom dipoles to the point charges. Colonna et al.[22] have recently reported their studies on modeling of electric field of formamide. The deficiences of using simple partial charge model has also been discussed in detail by these authors, and an overlap multipole expansion (OME) technique has been proposed to compute the electric field up to the hexadecapole level. In this paper we return to the atomic point charge approximation. This is the current standard because the point charge model provides a simple, fast approach to calculate the electrostatic interactions, and the efficiency of energy computation is still a major concern of molecular dynamics simulations. The current work in multipole moments in the literature including that discussed in the previous paper is undoubtedly the forerunner of next generation of force fields which use more rigorous description of electronic distribution.

In order to obtain transferable parameters, charges are further written as a sum of bond increments δ_{ij}, which indicates a charge transfer from atom i to atom j. For each atom i, the charge is a sum of all δ_{ij}, where j runs over all atoms that are directly

(19) Hehre, W. J.; Ditchfield, R.; Pople, J. A. *J. Chem. Phys.* **1972**, *56*, 2257. Hariharam, P. C.; Pople, J. A. *Theor. Chim. Acta* **1973**, *28*, 213. The 6-31G* basis set was used, which has been implemented in TURBOMOLE program (see references of preceding paper[1] 1), is slightly different from the conventional one. Instead of six, five d polarization functions ($d_{3z^2-r^2}$, $d_{x^2-y^2}$, d_{xy}, d_{yz}, d_{zx}) are employed.

(20) Williams, D. E. *Biopolymers* **1990**, *29*, 1367.
(21) Colonna, F.; Ángyán, J. G.; Tapia, O. *Chem. Phys. Lett.* **1990**, *172*, 55.
(22) Colonna, F.; Evleth, E.; Ángyán, J. G. *J. Comput. Chem.* **1992**, *13*, 1234.
(23) Urban, H. J.; Famini, G. R. *J. Comput. Chem.* **1993**, *14*, 353.
(24) Dinur, U.; Hagler, A. T. *J. Chem. Phys.* **1989**, *91*, 2949.

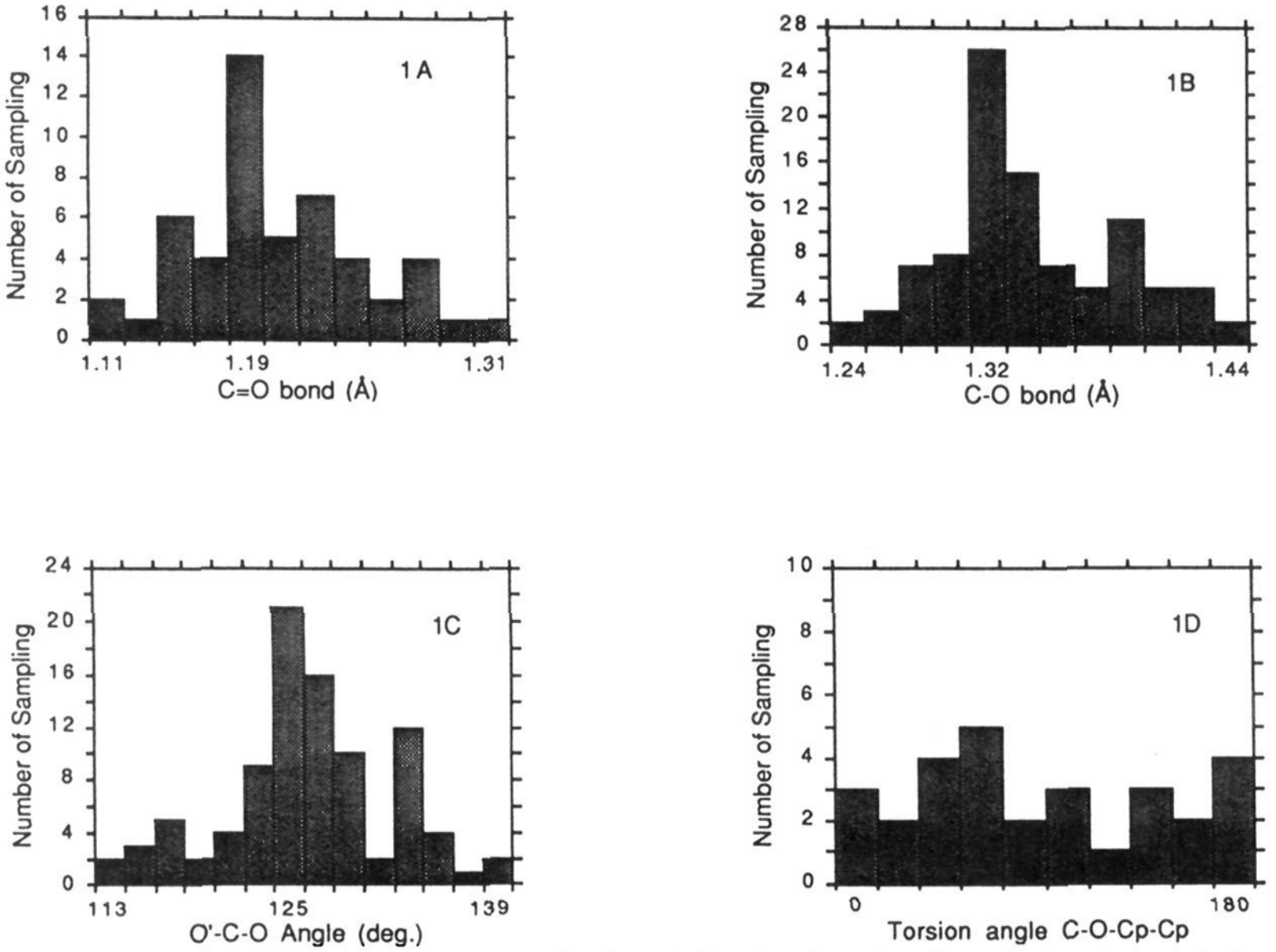

Figure 1. An example of degree to which the quantum energy surface is sampled in various internal coordinates for the carbonate molecules. In A and B, the range of carbonate $C_{carbonyl}$–$O_{carbonyl}$ and $C_{carbonyl}$–O_{ester} bond distances sampled are given. In C, the range of distortions of the carbonate $O_{carbonyl}$–$C_{carbonyl}$–O_{ester} angles is given, while in D, the range of torsion angles $C_{carbonyl}$–O_{ester}–C_{phenyl}–C_{phenyl} is given. These indicate the energy surface of the molecules are covered extremely well with bond ranges of 0.2 Å, angles of roughly 26°, and torsion angles over the whole range.

bonded to atom i

$$q_i = \sum_j \delta_{ij} \tag{3}$$

Among these three categories of energy contributions, nonbonded interactions are probably the most difficult to parameterize. One of the primary reasons for this is that one may not simply use the same methodology as for the intramolecular interactions because the Hartree–Fock approximation excludes dispersion energies, so this information may not be obtained directly from SCF *ab initio* calculations.

However, it is imperative that an adequate representation of the nonbonded interactions be obtained, because these interactions, in addition to the torsion contributions to the potential function, are of prime importance in determining the properties of synthetic polymers. To this end, the following pragmatic strategy has been adopted: First, as described in the previous paper, a set of effective charges are calculated by fitting to HF/6-31G* electrostatic potentials, which gives an approximate representation of the electrostatic interactions within the atomic point charge model. Because the charges from *ab initio* calculations with moderate basis sets usually do not reproduce the experimental electrostatic properties, such as dipole and quadrupole moments, the *ab initio* charges need to be scaled. The scaling factor and the van der Waals parameters are determined by fitting to crystal structures. Next, the valence parameters (parameters associated with bonds, angles, torsions, out-of-plane, and cross terms) are calculated by fitting to the *ab initio* data with both the charges and the van der Waals parameters held fixed. For the same reason as stated above, the valence parameters are subsequently scaled by a set of factors[18] determined by scaling quantum force fields of a large number of organic compounds to experiment. Thus, there are no additional adjustable parameters involved in this step. Finally, the parameters are validated by performing molecular mechanics calculations on model compounds and comparing the results with the experimental data.

3. Ab Initio Energy Surface

The *ab initio* HF/6-31G* optimized structures of carbonic acid and its methyl and phenyl derivatives were distorted randomly along their normal mode coordinates. A total of 58 structures, including optimized and distorted configurations, were generated to sample the intramolecular potential energy surfaces up to about 3 kcal/mol per degree of freedom above the minimum, i.e., about 40 kcal/mol for carbonic acid, 60 kcal/mol for methyl carbonate, etc. However, the sampling was selectively controlled by varying the maximum distortion permitted for each type of internal. A maximum variation of 0.1 Å was allowed for bond lengths and 15° for valence angles. A roughly-normal distribution was produced for most bond and angle coordinates. Special attention was paid to the torsional modes. Roughly uniform sampling was performed over this degree of freedom because of the small energy differences with respect to the torsion angles. Finally, both the geometries and energies of the distorted structures were examined carefully. Any distorted structures that were physically unreasonable were removed from the sample list. The degree to which the internals were sampled is indicated in Figure 1 where we have plotted the frequency of occurence of given values of several internals in the distorted structures.

The nonbonded energies are represented by interactions between any pair of atoms that are separated by three or more bonds (intramolecular interaction) or that belong to different molecules (intermolecular interaction). These refer both to electrostatic and van der Waals terms. The atomic partial charges derived from the electrostatic potential (ESP)[1] for the minimum

Table 1. Crystal Parameters for Ethylene Carbonate and Diphenyl Carbonate of 2,2-Bis(4-hydroxyphenyl)propane

	expt[a]	calc[b]	deviation
	Ethylene Carbonate		
a (Å)	8.92	8.96	0.04
b (Å)	6.25	6.32	0.07
c (Å)	6.94	6.97	0.03
α (deg)	90.0	90.0	0.0
β (deg)	100.3	98.2	-2.1
γ (deg)	90.0	90.0	0.0
	Diphenyl Carbonate		
a (Å)	18.86	18.65	-0.21
b (Å)	6.39	6.17	-0.22
c (Å)	10.56	10.27	-0.29
α (deg)	90.0	90.0	0.0
β (deg)	110.6	108.2	-2.4
γ (deg)	90.0	90.0	0.0

[a] Crystal structures, taken from refs 26 and 27. [b] Minimization results based on the force field.

Table 2. Calculated Lattice Energies (kcal/mol) of Ethylene Carbonate and Diphenyl Carbonate of 2,2-Bis(4-hydroxyphenyl)propane

	initial[a]	final[b] (diff)
	hskip 2.0 in Ethylene Carbonate	
$E_{ELEC.}$ (kcal/mol)	-7.7	-6.9 (0.8)
E_{VDW} (kcal/mol)	-15.3	-17.1 (-1.8)
E_{TOTAL} (kcal/mol)	-23.0	-24.1 (-1.1)
	hskip 2.0 in Diphenyl Carbonate	
$E_{ELEC.}$ (kcal/mol)	-3.8	-3.8 (0.0)
E_{VDW} (kcal/mol)	-60.6	-62.9 (-2.2)
E_{TOTAL} (kcal/mol)	-64.5	-66.7 (-2.3)

[a] Calculated on the structures taken from the experimental data, refs 26 and 27. [b] Optimized results via the force field.

energy structures of carbonic acid, dimethyl carbonate, and monophenyl carbonate were averaged and converted to bond increments δ_{ij}. Following Lifson et al.,[25] we derived the van der Waals parameters by fitting crystal structures, in this case, ethylene carbonate[26] and diphenyl carbonate of 2,2-bis(4-hydroxyphenyl)propane.[27] The intermolecular interactions were decoupled from intramolecular interactions by freezing all internal coordinates at their equilibrium values during the fitting procedure. The parameters were validated by performing lattice minimizations, and the results are given in Tables 1 and 2. The optimized lattice parameters are compared with experimental data, and the energies are partitioned into electrostatic and van der Waals contributions for both experimental and optimized structures. One can see that the calculation results are generally satisfactory. These were then used in the derivation of the valence parameters as described below.

For each of the distorted structures, *ab initio* HF/6-31G* calculations were conducted to obtain the total energies, gradients, and Hessian matrices. These quantities, together with the same quantities calculated for the optimized conformers, were used in a nonlinear least-squares fit to generate the force field parameters. Most parameters for alkyl and phenyl groups were derived separately[28] and transferred, except the phenyl ring coupling terms that are only available from 2,2-diphenylpropane. Nonbonded parameters were also frozen during the fitting procedure. Ill determined parameters, with very large standard deviations, mostly caused by redundancy, were set to zero. The results of fitting are summarized in Table 3, which lists several deviations of energy and energy derivatives for each of the model compounds.

(25) Lifson, S.; Hagler, A. T.; Dauber, P. *J. Am. Chem. Soc.* **1979**, *101*, 5111. Hagler, A. T.; Lifson, S.; Dauber, P. *J. Am. Chem. Soc.* **1979**, *101*, 5122.
(26) Brown, C. J. *Acta Crystallogr.* **1954**, *7*, 92.
(27) Perez, S.; Scaringe, R. P. *Macromolecules* **1987**, *20*, 68. Henrichs, P. M.; Luss, H. R.; Scaringe, R. P. *Macromolecules* **1989**, *22*, 2731.
(28) Hwang, M.; Maple, J. R.; Hagler, A. T., to be published.

Table 3. Deviations of the Energies and Energy Derivatives from a Least-Squares Fit of the Force Field[a]

	carbonic acid	methyl carbonate	dimethyl carbonate	phenyl carbonate	diphenyl isoprop
av δE	0.27	0.24	0.23	0.44	0.39
RMS δE	0.32	0.32	0.33	0.54	0.50
max δE	0.68	0.67	0.56	1.14	1.05
% grad[b]	6.88	10.42	11.35	11.78	16.49
% Hessian[c]	3.62	5.80	2.93	4.30	7.81

[a] Energies are in kcal/mol. [b] Relative deviations of the first derivatives of the total energies. [c] Relative deviations of the second derivatives of the total energies.

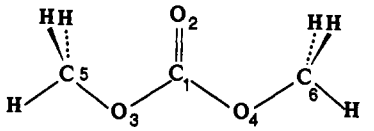

Figure 2. Illustration of the trans–trans minimum energy structure of dimethyl carbonate. Atom types used in the force field are given.

The data reveals that the fit was generally good. For example, the values of root mean square deviation of total energy (RMS δE) are less than 0.54 kcal/mol overall, for total energies ranging from 0 to over 100 kcal/mol. The largest maximum deviation of total energy is 1.14 kcal/mol for phenyl carbonate, and a detailed analysis related this value to a total energy of 62.0 kcal/mol. The relative deviation of gradients is generally larger than that of Hessians because some structures are close to the minimum energy structure and have very small gradients.

The valence parameters were then scaled by a standard set of scaling factors[28] that have been determined from comparisons between *ab initio* calculations and experimental data for a large number of organic molecules, including alkanes, acids, alcohol, aldehydes, ketones, amides, esters, etc.[28] The bond increments were also scaled. The final force field parameters of carbonate functional group ROCOOR, except alkane and phenyl ring parameters which are published elsewhere,[28] are given in Table 10. Angstroms and degrees are used for bond lengths and angles, respectively. The force constants are given in such a way that the energy calculated is in kcal/mol. Seven atom types are defined and listed in the first section of the table. Note that anharmonic force constants (cubic and quartic terms in the Taylor expansion) are given for bond and angle interactions. Most torsion interactions in this limited set of molecules may be represented by 1- and 2-fold terms. Some rotations are described by a single function due to symmetry, e.g., a 2-fold function for rotations about a double bond in a phenyl ring, a 3-fold function for rotation of a methyl group, and a 4-fold function for a phenyl ring rotation in the diphenyl isopropane segment. However, the actual energy curve of rotation about a particular bond is a combination of all relevant rotation functions and nonbonded interactions. Two out-of-plane interactions are represented by harmonic functions. Coupling terms and nonbonded parameters are also given in this table.

4. Molecular Mechanics Calculations and Discussion

Molecular mechanics (MM) calculations were carried out on several molecular systems to test the force field parameters and to probe structural and energetic properties of carbonates.

(1) Dimethyl Carbonate. Dimethyl carbonate (Figure 2) is the smallest stable carbonate molecule. Its equilibrium structure has been extensively studied by several groups using a variety of methods, including electron diffraction,[29] infrared and Raman spectroscopy,[30,31] and dielectric measurement.[32] The equilibrium structure in both the gas and liquid states has been found to be the trans–trans conformer with C_{2v} point group symmetry (Figure 2). Infrared and Raman spectra determined[30] on a liquid sample indicated that a trans–cis conformer with C_s point group also

(29) Mijlhoff, F. G. *J. Mol. Struct.* **1977**, *36*, 334.

Table 4. Relative Energies and Geometrical Parameters for Optimized Structures of Dimethyl Carbonate

	trans–trans		trans–cis	
	FF[a]	HF/6-31G*	FF[a]	HF/6-31G*
		Internals		
C_1–O_2 (Å)	1.19	1.19	1.19	1.18
C_1–O_3 (Å)	1.32	1.31	1.31	1.32
C_1–O_4 (Å)	1.32	1.31	1.31	1.32
O_3–C_5 (Å)	1.42	1.42	1.42	1.42
O_4–C_6 (Å)	1.42	1.42	1.42	1.42
$\angle O_2C_1O_3$ (deg)	125.8	125.4	125.3	124.7
$\angle O_2C_1O_4$ (deg)	125.8	125.4	120.6	122.7
$\angle C_1O_3C_5$ (deg)	115.9	116.4	115.8	116.3
$\angle C_1O_4C_6$ (deg)	115.9	116.4	125.9	121.2
		Energies		
ΔE (kcal/mol)	0.0	0.0	3.8	3.7 3.3[b]

[a] Calculated with the force field. [b] MP2/6-31G*//HF/6-31G* results.

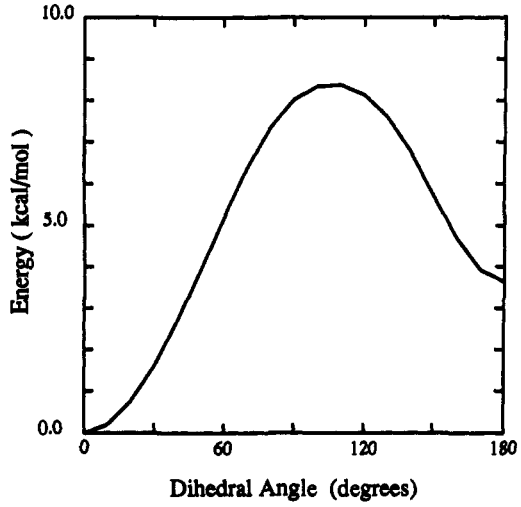

Figure 3. Minimum energy curve of the internal rotation about one C–O bond of dimethyl carbonate. The dihedral angle is defined as that of O_2–C_1–O_3–C_5 (Figure 1). The trans–trans conformer corresponds to 0° and the trans–cis conformer corresponds to 180°.

exists. Both trans–trans and trans–cis geometries were optimized using the force field developed, and the geometrical parameters and relative energies corresponding to these structures are given in Table 4, together with the HF/6-31G* results. One sees that the MM results agree well with those of the *ab initio* computations, especially for the minimum energy structure. The energy difference between these two conformers predicted by the force field is 3.7 kcal/mol, which is also in good agreement with the energy difference of 3.8 kcal/mol from the HF/6-31G* calculation and that of 3.3 kcal/mol obtained using the MP2/6-31G* method with the HF/6-31G* optimized structures.[1] The zero point energy difference, which is estimated based on the harmonic approximation, further lowers the energy difference by 0.1 kcal/mol. Note these values are in reasonably good agreement with the enthalpy difference of 2.6 ± 0.5 kcal/mol, estimated from the temperature dependency of the liquid-state IR spectroscopy.[30] A minimum energy transition path between these two conformers was calculated by forcing the torsion angle in 10° increments while optimizing all other internal coordinates, and the result is plotted in Figure 3. The energy maximum occurs at approximately 100° and the barrier height is 8.4 kcal/mol.

Normal mode vibrational frequencies were calculated and are listed in Table 5. In the same table, we also list the results obtained from the HF/6-31G* calculations, from the quantum mechanical force field (which is the force field before the final scaling), and experimental values measured in the liquid[30] and vapor[31] states.

(30) Katon, J. E.; Cohen, M. D. *Can. J. Chem.* **1975**, *53*, 1378.

Table 5. Normal Mode Vibrational Frequencies of Dimethyl Carbonate (cm^{-1})[a]

approx mode	C_{2v} symm spec	SCF[b]	QMFF[c]	FF[d]	expt[e]	expt[f]
νCH_3(asym)	a1	3355(327)	3313(258)	2993(–35)	3028	3032
νCH_3(sym)	a1	3254(293)	3233(272)	2910(–51)	2961	2964
$\nu C=O$	a1	2003(243)	2007(247)	1769(9)	1760	1774
δCH_3(asym)	a1	1651(193)	1629(171)	1509(51)	1458	1414
δCH_3(sym)	a1	1625(189)	1661(225)	1463(27)	1436	1458
δCH_3(rock)	a1	1371(162)	1371(162)	1227(18)	1209	1195
νOCO(sym)	a1	1288(168)	1268(148)	1114(–6)	1120	1116
νCH_3–O	a1	1038(122)	993(77)	912(–4)	916	922
δOCO	a1	558(40)	545(27)	501(–17)	518	857
δOCO	a1	255(–2)	231(–26)	242(–15)	257	518
νCH_3(asym)	a2	3336(329)	3315(308)	2989(–18)	3007	3004
δCH_3(asym)	a2	1644(191)	1645(191)	1466(13)	1453	1432
δCH_3(rock)	a2	1300(110)	1289(99)	1174(–16)	1190	1234
CH_3O(tors)	a2	224(26)	285(87)	220(22)	198	
CH_3(tors)	a2	149(13)	162(26)	134(–2)	136	
νCH_3(asym)	b1	3355(327)	3313(258)	2993(–35)	3028	3032
νCH_3(sym)	b1	3253(293)	3233(272)	2910(–51)	2961	2965
δCH_3(asym)	b1	1658(200)	1667(209)	1509(51)	1458	1414
δCH_3(sym)	b1	1648(212)	1631(195)	1480(44)	1436	1458
νOCO(asym)	b1	1505(226)	1527(248)	1293(14)	1279	1299
δCH_3(rock)	b1	1337(128)	1341(132)	1211(2)	1209	1160
νCH_3–O	b1	1109(136)	1078(105)	962(–11)	973	989
δOCO_2(rock)	b1	773(83)	760(68)	696(4)	692	634
δOCO	b1	379(7)	329(43)	355(–17)	372	579
νCH_3(asym)	b2	3336(329)	3315(308)	2989(–18)	3007	3004
δCH_3(asym)	b2	1645(187)	1645(187)	1480(22)	1458	1432
δCH_3(rock)	b2	1303(138)	1289(124)	1174(9)	1165	1210
δOCO_2(rock)	b2	905(108)	943(146)	831(34)	797	801
CH_3O(tors)	b2	172(–26)	193(–5)	177(–21)	198	–
CH_3(tors)	b2	126(–10)	131(–5)	92(–44)	136	–

[a] Differences between calculated results and experimental values are given in parentheses. [b] Results from quantum mechanical SCF calculation with 6-31G* basis set. [c] Calculated based on the quantum mechanical force field. [d] Calculated based on the force field. [e] Liquid state, ref 30. [f] Vapor state, ref 31.

There is some disagreement between the gas- and liquid-state experimental data, mainly due to misassignments in early work by Collingwood et al.,[31] who assumed that only the trans–trans structure existed in the system. Other than that, most frequencies in the liquid state are very close to their counterparts in the vapor state, indicating that the intermolecular interactions in these systems are weak. Consequently, a valid comparison may be made between the vibrational frequencies calculated in the current work and the more complete liquid-state experimental data.

This is a good example with which to illustrate the validity of using the scaling factors that were transferred from independent studies[30] and that are utilized to scale the *ab initio* force field parameters. One can see that the quantum mechanical force field basically reproduces the *ab initio* results with the maximum deviation between these two sets of calculated frequencies of only about 60 cm^{-1}. However, the results are significantly shifted from the experimental values, and by applying the previously determined scale factors with no additional parametrization a set of frequencies is obtained that is in good agreement with the experimental results.

(2) Diphenyl Carbonate. The minimum energy structure of diphenyl carbonate is a trans–trans conformer with C_2 symmetry, and both phenyl rings twisted out of the OCOO plane by about 60°, as illustrated in Figure 4. Several geometrical parameters are given in Table 6.

Calculations based on the force field show that the trans–cis conformer of diphenyl carbonate is 2.6 kcal/mol higher in energy than the minimum energy trans–trans conformer and that the barrier height for the transition from trans–trans to trans–cis is 6.3 kcal/mol, which is 2.1 kcal/mol lower than the barrier height

(31) Collingwood, B.; Lee, H.; Wilmshurst, J. K. *Aust. J. Chem.* **1966**, *19*, 1637.

(32) Labrenz, D.; Schröer, W. *J. Mol. Struct.* **1991**, *249*, 327.

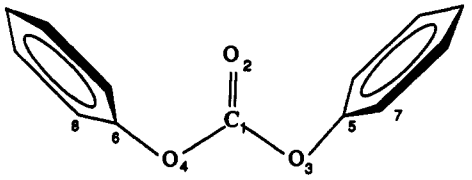

Figure 4. Illustration of the trans–trans minimum energy conformer of diphenyl carbonate. Both rings are twisted in an opposite sense by about 60°. The molecule has C_{2v} symmetry. The atom types that are used in the force field are given except the phenyl carbons which are denoted as C_p in the force field.

Table 6. Relative Energies and Geometrical Parameters for Optimized Structures of Diphenyl Carbonate

	trans–trans		trans–cis	
	FF[a]	HF/6-31G* [b]	FF[a]	HF/6-31G* [b]
		Internals		
C_1–O_2 (Å)	1.19	1.19	1.19	1.19
C_1–O_3 (Å)	1.32	1.32	1.32	1.32
C_1–O_4 (Å)	1.32	1.32	1.32	1.32
O_3–C_5 (Å)	1.39	1.39	1.39	1.39
O_4–C_6 (Å)	1.39		1.38	
$\angle O_2C_1O_3$ (deg)	126.3	126.9	119.8	122.5
$\angle O_2C_1O_4$ (deg)	126.3	126.9	125.4	122.7
$\angle C_1O_3C_5$ (deg)	119.3	119.8	128.8	124.3
$\angle C_1O_4C_6$ (deg)	119.3		119.3	
ψ_1 (deg)	60.5	63.5	68.1	90.0
ψ_2 (deg)	60.5		52.1	
		Energies		
ΔE (kcal/mol)	0.0	0.0	2.6	2.5

[a] Results calculated via the force field. [b] The ab initio results are for monophenyl carbonate.

in dimethyl carbonate. This can be explained by the fact that the repulsion between the phenyl and the carbonyl (C=O) groups is stronger than the repulsion between the methyl and the carbonyl groups in the trans–trans conformer. Thus, the trans–trans conformation is somewhat more unstable relative to the minimum energy structure in the case of diphenyl carbonate than in the case of dimethyl carbonate. This explanation is supported by MM calculations performed by the authors on carbonic acid. The transition barrier height in carbonic acid is 8.6 kcal/mol, which is 0.2 kcal/mol higher than the height of the barrier for dimethyl carbonate.

The motions of phenyl rings in the diphenyl carbonate molecule were studied by calculating the minimum energy transition curves with respect to the dihedral angle ϕ as defined by atoms C_1–O_3–C_5–C_7 (see Figure 4). As illustrated by the solid curve in Figure 5, the rotational barrier is about 1.5 kcal/mol at $\phi = 0°$ and 180° when the molecule is planar, and 0.18 kcal/mol at $\phi = 90°$ when one of the rings is perpendicular to the $O_3C_1O_2O_4$ plane. Both values are slightly larger than the SCF results but close to those obtained from the MP2/6-31G*//HF/6-31G* calculations.[1] Also in Figure 5, the energy contribution from torsion terms only is plotted as well as the difference between the total energy and the torsional energy, denoted as "other" in the figure. This clearly shows that the rotation energy curve is a combination of two opposing contributions. Torsional terms favor the planar structure so that a larger conjugated system may be formed and so that the delocalization of electrons may lower the total energy, but the other terms, mostly nonbonded interactions, favor the perpendicular conformation so that the repulsions between the phenyl groups and carbonyl group can be minimized. The combined result is a minimum energy structure having a partly twisted ($\phi \simeq 60°$) conformation.

Information regarding the extent of coupling between the two phenyl rings in diphenyl carbonate may also be obtained from Figure 5. As one phenyl ring is rotated about the O–C_p bond, the position of the other ring remains in its equilibrium position. Thus, this molecule does not maintain C_2 symmetry as this rotation

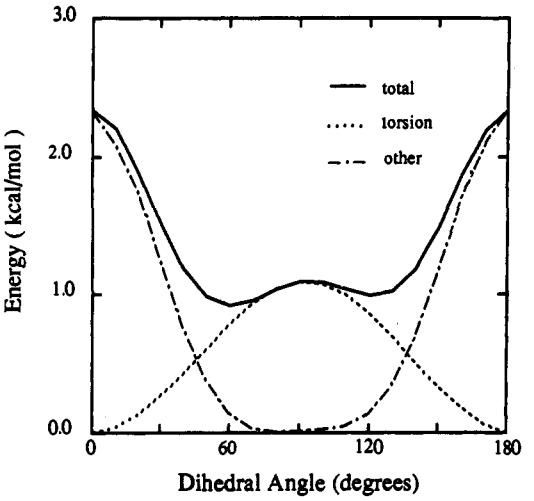

Figure 5. Minimum energy curves for rotation of a phenyl ring in diphenyl carbonate about the dihedral angle C_1–O_3–C_5–C_7. The total energy is partitioned into two contributions: "torsion" and "other". The torsion function favors the planar structure (0° or 180°), while the other terms, mostly nonbonded interactions, prefer a twisted structure (90°).

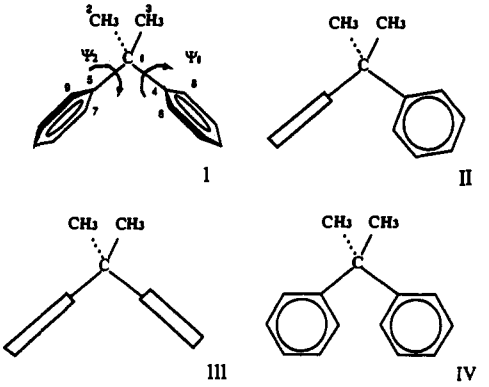

Figure 6. Illustration of the energy minimized structures of 2,2-diphenylpropane. The minimum energy structure is denoted as I, which has both rings twisted out of the plane by about 50°. The torsion angles ψ_1 and ψ_2 in the text are defined by the atoms C_5–C_1–C_4–C_6 and C_4–C_1–C_5–C_7.

proceeds, which explains why an asymmetric double well potential curve is obtained in Figure 5. The local minimum at $\simeq 120°$, which is about 0.1 kcal/mol higher than the global minimum, corresponds to a parallel position of the two phenyl rings as they are twisted in the same direction by about 60°. Because the two phenyl groups are separated by three atoms, no valence interaction is involved between the two groups, and the coupling between the two rings is represented solely by nonbonded interactions, the magnitude of this nonbonded interaction is only about 0.1 kcal/mol in this case.

(3) 2,2-Diphenylpropane. Molecular mechanics calculations were performed on four conformers of 2,2-diphenylpropane (Figure 6) using the force field, and the results are summarized in Table 7. The conformational energy differences agree well with the results of HF/6-31G* and MP2/6-31G*//HF/6-31G* calculations.[1] The largest deviation, about 1 kcal/mol, occurs for structure IV with the MM result giving the higher energy. The geometrical parameters reproduce the dramatic changes observed with the *ab initio* results for all four structures; even in the case of structure IV. For instance, on going from structure I to structure IV, the angle $\angle C_5C_1C_4$ expands from 110.7° to 122.8°, while the *ab initio* HF/6-31G* results reveal a change from 110.0° to 121.8°. This shows that large changes in valence coordinates may accompany conformational changes. The force field reported here has the flexibility to reflect such a change.

The coupling between the two phenyl groups is much stronger than is the case for diphenyl carbonate. This is clearly illustrated

Table 7. Relative Energies and Geometrical Parameters for Optimized Structures of 2,2-Diphenylpropane

	I		II		III		IV	
	FF	HF/6-31G*	FF	HF/6-31G*	FF	HF/6-31G*	FF	HF/6-31G*
				Internals				
C_1–C_2 (Å)	1.54	1.54	1.54	1.55	1.54	1.55	1.54	1.54
C_1–C_3 (Å)	1.54	1.54	1.54	1.55	1.54	1.55	1.55	1.54
C_1–C_4 (Å)	1.54	1.54	1.54	1.54	1.53	1.54	1.57	1.56
C_1–C_4 (Å)	1.54	1.54	1.55	1.54	1.53	1.54	1.57	1.56
$\angle C_2C_1C_3$ (deg)	107.3	107.3	106.1	107.1	102.0	104.5	109.4	110.4
$\angle C_4C_1C_5$ (deg)	110.7	110.0	112.4	111.1	112.2	109.0	122.8	121.8
ψ_1 (deg)	50.5	50.5	0.0	0.0	90.0	90.0	0.0	0.0
ψ_2 (deg)	50.5	50.5	90.0	90.0	90.0	90.0	0.0	0.0
				Energies				
ΔE (kcal/mol)								
HF/6-31G*	0.0	0.0	2.1	2.2	3.9	3.9	18.2	17.2
MP2/6-31G*//HF/6-31G*		0.0		1.8		4.0		16.8

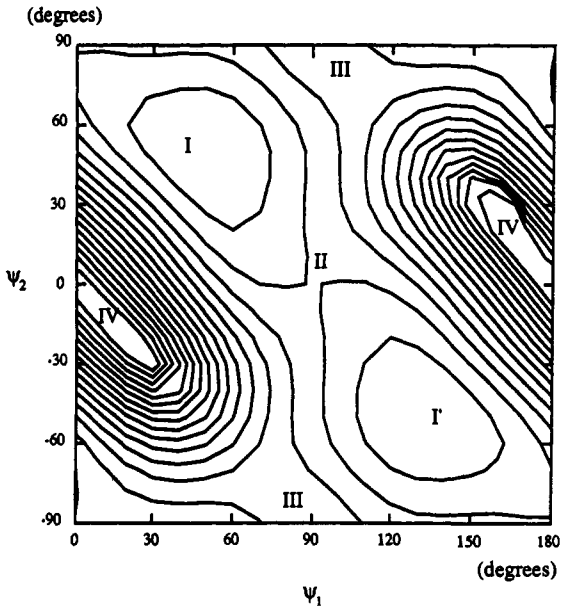

Figure 7. Minimum energy map for the two dihedral angles ψ_1 and ψ_2 in 2,2-diphenylpropane. The interval is 1 kcal/mol. I and I' indicate two identical minimum energy structures that can be linked by two possible transition paths through structure II or structure III, respectively. The most favorable transition energy barrier is about 2.1 kcal/mol which corresponds to the path through structure II where one angle is 90° and the other is 0°.

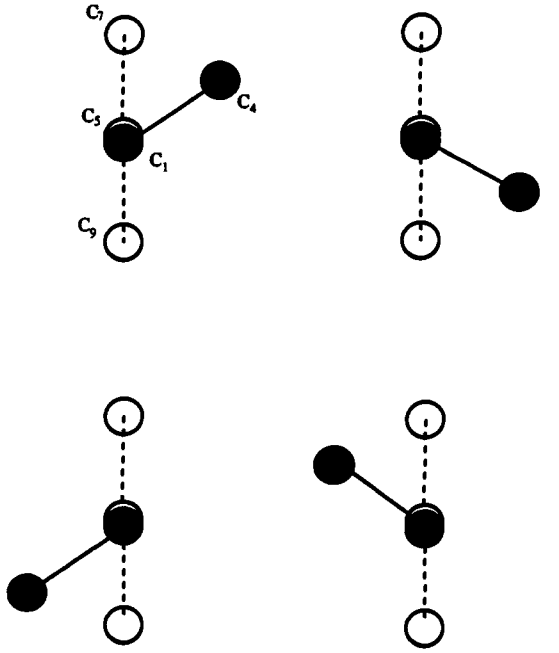

Figure 8. Four degenerate structures of 2,2-diphenylpropane as the dihedral angle C_7–C_5–C_1–C_4 changes from 0° to 360°. The C_5–C_1 bond is perpendicular to the plane of the paper. Black dots denote atoms above the plane of the paper and circles denote atoms below the plane of the paper.

by the optimized internal rotation energy map plotted in Figure 7. Again, this map was obtained by optimizing all other degrees of freedom, while the two torsion angles (ψ_1 and ψ_2 are defined as dihedral angles of C_5–C_1–C_4–C_8 and C_4–C_1–C_5–C_7 respectively, as illustrated in Figure 6) were fixed at given values. Due to symmetry, this map covers only a 180° range. Although this figure may be incomplete as the figure does not represent a total systematic search of all minima with respect to the methyl rotation, but rather a projection into two dimensions, it still provides important information. It is an adiabatic surface and the contours show some important features of phenyl-ring motion that has long been considered as one of the most important dynamic properties of polycarbonates.[2-5]

There are two minima in this map, denoted by I and I', which correspond to conformer I in Table 7. Between these two minima, one can draw a line that either crosses the saddle point labeled II or that labeled III; both indicate possible transition paths. The coupling between the two rings is so strong that, in order to maintain a relatively low energy, if one ring is rotated the other ring must undergo a sympathetic rotation. If one torsion angle is fixed at its minimum energy value, the transition barrier height of the other angle is more than 10 kcal/mol. However, synchronous rotation of the two phenyl rings can dramatically reduce the transition barrier. The most favorable transition path is through structure II, which has a barrier height of 2.1 kcal/mol. This path corresponds to a coherent rotation of the two rings in the same direction, such that an approximately constant relative position is maintained between these two rings during the transition. The second most favorable path is through conformer III, for which the barrier height is 3.9 kcal/mol. In this case, the two rings rotate in an opposite sense.

In order to reproduce the *ab initio* potential energy surface of the two phenyl ring motions in diphenyl propane, a 4-fold function

$$k_4(1 - \cos 4\psi) \qquad (4)$$

was used, which corresponds to the entry of torsion C_p–C_p–C–C_p given in the force field file (Table 10). This reflects the symmetry requirements that there are four identical structures as the torsion angle ψ changes from 0° to 360°, as illustrated in Figure 8. The 4-fold function causes energy minima to occur at torsion angles of ±45° and ±135°. The small difference between these values and the actual minimum energy torsional angles is caused by nonbonded repulsions between the two phenyl rings.

(4) Diphenyl Carbonate of 2,2-Bis(4-hydroxyphenyl)propane. Diphenyl carbonate of 2,2-bis(4-hydroxyphenyl)propane (Figure

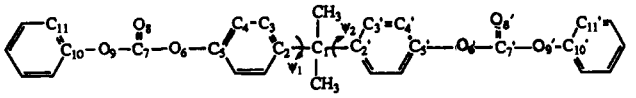

Figure 9. Illustration of diphenyl carbonate of 2,2-bis(4-hydroxyphenyl)-propane.

Table 8. Comparison of Calculated and Crystal Parameters for the Diphenyl Carbonate of 2,2-Bis(4-hydroxyphenyl)propane[a]

	calc[b]	crystal[c]
Bond Lengths (Å)		
C_7–O_8, $C_{7'}$–$O_{8'}$	1.19, 1.19	1.17, 1.15
C_7–O_6, $C_{7'}$–$O_{6'}$	1.32, 1.32	1.33, 1.33
C_7–O_9, $C_{7'}$–$O_{9'}$	1.32, 1.32	1.33, 1.34
O_6–C_5, O_6–$C_{5'}$	1.40, 1.40	1.41, 1.42
O_9–C_{10}, $O_{9'}$–$C_{10'}$	1.40, 1.40	1.41, 1.40
Bond Angles (deg)		
O_8–C_7–O_6, $O_{8'}$–$C_{7'}$–$O_{6'}$	126.3, 126.3	126.1, 127.0
O_8–C_7–O_9, $O_{8'}$–$C_{7'}$–$O_{9'}$	126.4, 126.4	127.3, 127.5
C_7–O_6–C_5, $C_{7'}$–$O_{6'}$–$C_{5'}$	119.0, 119.0	115.4, 117.2
C_7–O_9–C_{10}, $C_{7'}$–$O_{9'}$–$C_{10'}$	119.3, 119.3	119.3, 116.8
Torsion Angles (deg)		
C_7–O_6–C_5–C_4, $C_{7'}$–O_6–$C_{5'}$–$C_{4'}$	60.9, 60.9	89.2, 89.0
C_7–O_9–C_{10}–C_{11}, C_{7m}–$O_{9'}$–$C_{10'}$–$C_{11'}$	62.0, 62.0	48.0, 77.6
C_1–C_2–C_3–C_4, C_1–C_2–C_3–$C_{4'}$	50.7, 50.7	61.3, 35.9

[a] Atom numbers are given in Figure 8. [b] Results of single molecule, calculated via the force field. [c] Crystal data.[27]

9) is a structural analogue of BPAPC. Calculations performed on an isolated molecule show that the optimized structure has C_2 symmetry. The energetic and geometrical properties are very close to those calculated for the smaller model molecules, diphenyl carbonate and 2,2-diphenylpropane. Some of the optimized geometrical parameters are given in Table 8, together with crystal data.[27] At least two crystal structures are known for this molecule. They are referred to as the mobile and immobile forms,[27] because ring flipping is known to be facile in the former but not the latter. The geometrical data of just the immobile form are included in Table 8 for comparison because more complete experimental data are given.[27] It is apparent that the molecules in the crystal do not maintain the intrinsic molecular C_2 symmetry, as indicated by different values for each of the internals reported (Table 8). This is once again a case where crystal packing clearly affects the conformation of the molecules.

Comparison of data given in Table 8 indicates that most bond lengths and angles obtained for the isolated molecule via the force field are in good agreement with the crystal data.[27] However, the number and type of comparisons with experimental data are limited because the experiments are conducted on condensed phases, and it is inappropriate to directly compare properties that are sensitive to intermolecular interactions and calculated on isolated molecules with those measured in condensed phase. To further probe the qualitative effects of intermolecular interactions, we performed molecular mechanics calculations on the ring rotations in a crystal-like cluster of diphenyl carbonate of 2,2-bis(4-hydroxyphenyl)propane. The starting point of this calculation was taken from the crystal structure.[27] The cluster includes seven molecules in total; one molecule in the center surrounded by six others. With the outer six molecules constrained to match the experimental coordinates, the calculation was performed on the central molecule. It was torsion forced and minimized in the same manner as for the simulations on isolated molecules; while one torsional angle ψ_1 ($C_{2'}$–C_1–C_2–C_3, Figure 9) was forced to a given value, all other internal coordinates including ψ_2 (C_2–C_1–$C_{2'}$–$C_{3'}$, Figure 9) were allowed to relax during the minimization. The calculated relative energies in a range of 180° of the torsion angle ψ_1 are plotted out in Figure 10, together with, for comparison, the equivalent curve for an isolated molecule. One can see that these two curves are significantly different. The minimum in the curve for the isolated molecule is at about 50°,

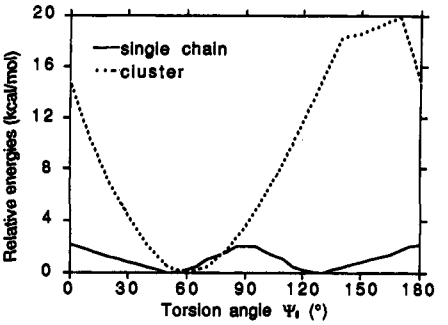

Figure 10. Minimum energy curves for the internal rotation angle C_3–C_2–C_1–$C_{2'}$ of diphenyl carbonate of 2,2-bis(4-hydroxyphenyl)propane, in an isolated molecule and in a crystal-like cluster.

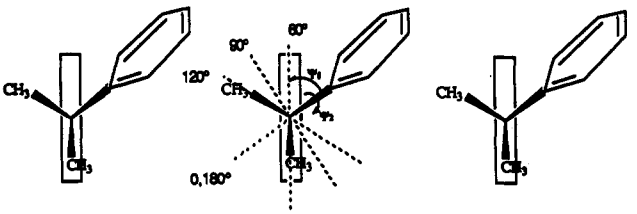

Figure 11. Newman projection along the C_1–C_2 bond of diphenyl carbonate of 2,2-bis(4-hydroxyphenyl)propane in the crystal (ref 22). The center front 2-propyl carbon atom has two methyl and one phenyl substituents. The phenyl ring that was torsion forced during the minimization is represented by the rear rectangle. The rotations are measured by the torsion angles ψ_1 and ψ_2.

but this occurs at about 60° for the molecule in the cluster, consistent with one of the experimentally determined angles. The rotational energy curve for the isolated molecule is symmetric about 90°. It has two minima separated by two transition states of identical barrier heights at both 0° and 90°. But in the cluster this symmetry is broken. In fact, a single barrier appears around $\psi_1 = 150°$. The barrier height, based on this very approximate calculation in a static environment, is about 20 kcal/mol.

A schematic illustration of the phenyl ring flipping motion in the crystal environment is given by a Newman projection along the C–C_{phenyl} bond in Figure 11. In the central molecule in Figure 11, the center front 2-propyl carbon atom has two methyl and one phenyl substituents. The phenyl ring that was torsion forced in represented by the rear rectangle. The two nearest molecules in the cluster are also plotted out in this figure. The phenyl ring rotations are measured by the torsion angles ψ_1 and ψ_2, as given in the figure. The minimum energy structure corresponds to 61.5° for both angles. In the isolated molecule case, these two torsional angles are coupled. When ψ_1 changes to 0°, ψ_2 moves to 90° to minimize the total energy, and vice versa. Consequently, there are four equivalent minimum energy structures corresponding to ±60° and ±120°. However, such a synchronous motion is not feasible in the crystal environment because the surrounding molecules break the symmetry of the ring rotations (as shown in Figure 11) and significantly increase the energetic cost of simultaneous rotation of the two rings.

Energy breakdown analyses were conducted for two conformers, $\psi_1 = 60°$ and 120°, of the ring flipping in the cluster. The results are given in Table 9. Examination of the energy components reveals that the total energy difference of 11.54 kcal/mol between these two conformers consists of contributions from both bonded and nonbonded interactions of 3.96 and 7.60 kcal/mol, respectively. Note that the bonded energy increment of 3.91 kcal/mol is largely from the torsion energy contribution of 3.94 kcal/mol. Further analysis shows that the nonbonded energy increment of 7.6 kcal/mol is mostly from the intermolecular VDW energy increment of 6.02 kcal/mol; the intramolecular VDW contribution to the difference is only 1.09 kcal/mol; and the changes of both intra- and intermolecular electrostatic interactions are small. These results are consistent with our intuition. As illustrated in

Table 9. Component Analysis of Potential Energies (in kcal/mol) for Two Rotational Conformers of Diphenyl Carbonate of 2,2-Bis(4-hydroxyphenyl)propane Cluster

ψ_1	60°	120°	$E_{120°} - E_{60°}$
	Bonded Energies		
E_{total} (bonded)	9.62	13.58	3.96
bond	6.66	7.62	0.97
angle	8.09	6.61	-1.48
tors.	1.19	5.13	3.94
outp	0.32	0.36	0.04
b/b	0.49	0.51	0.01
b/a	-0.23	-0.33	-0.10
a/a	-0.45	-0.37	0.08
b/t	-2.44	-2.82	-0.38
a/t	-3.94	-3.14	0.79
aat	-0.07	0.01	0.07
	Nonbonded Energies		
E_{total} (nonbonded)	-103.26	-95.66	7.60
inter			
VDW	-51.88	-45.86	6.02
Coulomb	-20.11	-20.31	-0.20
intra			
VDW	26.59	27.68	1.09
Coulomb	-57.86	-57.17	0.69
	Total Energies		
E_{total}	-93.64	-82.09	11.54

Figure 11, when one ring is twisted from $\psi_1 = 60°$ (minimum energy state) to $\psi_1 = 120°$, a serious steric crowding is created among the twisted ring and surrounding chains. The ring flipping in such an environment needs to overcome two major energy barriers: intrinsic torsion energy barrier and steric repulsions.

The rotational barrier height in glassy polycarbonates is a subject of continued investigation. The 20 kcal/mol barrier height calculated in the crystal-like cluster obviously overestimates this value because of the imposed rigidity and the closer crystalline packing. These results do indicate, however, that intermolecular interactions in a condensed phase can significantly affect the rotational energy profile, including both the barrier height and position. This phenomenon has also been noted recently by Hutnik et al.[17]

5. Conclusion

Based on *ab initio* HF/6-31G* calculations and known experimental data, an all atom force field has been developed for polycarbonates.

The valence parameters were obtained by fitting to the total energies and first and second derivatives of the total energies of a set of model molecules, which were distorted along their normal mode coordinates to sample the intramolecular interactions. Nonbonded parameters were derived from two sources: from *ab initio* calculations and by fitting to crystal structures. Atomic partial charges, which are used to represent the electrostatic interactions, were determined by fitting to electrostatic potentials calculated directly from the Hartree–Fock wave functions. Van der Waals parameters were obtained by fitting to crystal structures, during which process the charges were scaled and frozen. The force field parameters were scaled by a set of parameters to correct for the Hartree–Fock approximation. Calculations performed on dimethyl carbonate illustrate the success of this scaling. By including all degrees of freedom, the force field is more general and flexible than those that require parts of the molecule to be rigid. In particular, large changes in valence coordinates are found to accompany conformational changes and may be required to adequately account for the trends in energies of these structures.

Molecular mechanics calculations were performed to test and validate this force field, and the results agree well with the available quantum mechanical and experimental data. The importance of

Table 10. Force Field Parameters

I. Atom Types

C′	carbonyl carbon	C_p	phenyl carbon
O′	carbonyl oxygen	H	hydrogen bonded to C, C_p
O	ester oxygen	H*	hydrogen bonded to O
C	alkyl carbon		

II. Valence Parameters

bond	R_0	K_2^b	K_3^b	K_4^b
C′–O′	1.1953	854.2903	-1922.3407	2301.6824
C′–O	1.3398	391.3310	-788.5655	1212.3812
O–H*	0.9520	534.2994	-1287.1937	1889.1396
O–C	1.4177	326.7273	-608.5306	689.0333
O–C_p	1.3828	387.9119	-715.9186	660.2442

angle	θ_0	K_2^a	K_3^a	K_4^a
O′–C′–O	120.0510	97.3782	-26.5619	
0–C′–O	109.4930	137.9111	-39.8755	59.0768
C′–O–H*	113.1580	49.6892	-25.9467	
C′–O–C	113.6200	57.9274	-17.1312	
O–C–H	107.6880	70.4801	-10.3498	
C′–O–C_p	115.0700	47.1131	-32.5592	
O–C_p–C_p	120.1400	33.0391	-14.7807	
O–C–C	108.4100	63.3907	-13.4513	
C_p–C–C_p	112.7650	37.1564	-39.1209	

torsion	K_1^t	K_2^t	K_3^t	K_4^t
O′–C′–O–H*	-3.0147	1.6536		
0–C′–O–H*	-3.0513	1.6679		
O′–C′–O–C	-4.2342	1.8099		
O–C′–O–C	-4.0149	1.8643		
C′–O–C–H			-0.1932	
O′–C′–O–C_p	-3.4253	2.3292		
O–C′–O–C_p	-3.2773	1.3788		
C′–O–C_p–C_p	-2.4045	0.4561		
O–C_p–C_p–H		2.1670		
O–C_p–C_p–C_p		4.6282		
C_p–C–C_p–C_p				-0.1500

out-of-plane	K^o	out-of-plane	K^o
O′–C′–O–O	51.6374	O–C_p–C_p–C_p	19.8126

III. Cross Term Parameters

bond–bond		bond–bond	
O′–C′–O	122.4966	C′–O–C_p	69.5999
O–C′–O	83.7102	O–C_p–C_p	30.3889
C′–O–H*	16.9326	O–C–C	23.2647
C′–O–C	42.0941		

bond–bond	left bond	right bond	bond–bond	left bond	right bond
O′–C′–O	73.6008	81.8533	C′–O–C_p	64.3958	39.1599
O–C′–O	102.6457	102.6457	O–C_p–C_p	83.6766	49.6672
C′–O–H*	41.3971	19.6376	O–C–C	57.9487	45.3326
C′–O–C	53.5920	32.4816	C_p–C–C_p	15.0313	15.0313
O–C–H	57.4975	8.6864			

angle–angle		angle–angle	
O′–C′–O/O–C′–O	23.5619	H–C–O/O–C–C	14.3133
H–C–O/O–C–H	13.9120	O–C–H/H–C–C	12.8080
O–C–H/H–C–H	8.4115		

bond–torsion	K_1	K_2	K_3	bond–torsion	K_1	K_2	K_3
O′–C′–O–H*		4.6500		O–C′–O–C		12.4736	
O–C′–O–H*		6.4376		O′–C′–O–C_p		4.9491	
O′–C′–O–C		4.6748					

	left			right		
angle–torsion	K_1	K_2	K_3	K_1	K_2	K_3
O′–C′–O–H*	-5.1252	2.5207		7.7354		
O–C′–O–H*		3.3455		6.4470		
O′–C′–O–C	-5.4740	2.1378		14.5110		
O–C′–O–C	-4.6620	4.1706		13.0437	-1.4577	
C′–O–C–H		-1.9980		-4.7254		
O′–C′–O–C_p	-5.8982	6.4425		6.4547		
O–C′–O–C_p	-1.8200	3.1430		2.7587	2.4717	

IV. Nonbond Parameters

	r	ϵ		r	ϵ
C′	4.0100	0.0640	O	3.6890	0.2400
O′	2.9000	0.2670	H*	1.8000	0.0500

	$\delta_{i,j}$		$\delta_{i,j}$
C′–O′	0.4477	C–O	0.2630
C′–O	0.0868	C_p–O	0.1711
H*–O	0.3549		

intermolecular interactions in the ring flipping motion was shown by the calculations on a crystal-like cluster. More detailed investigations of phenyl ring rotations in BPAPC as well as other applications of the force field to the computer simulation of polycarbonates are underway.

Acknowledgment. This work was supported as part of Biosym Technologies' Polymer Project, which is funded by a consortium of 50 companies and government laboratories. One of the authors, H.S., thanks Professor B. E. Eichinger and Professor R. O. Watts for beneficial discussions and encouragement.